NACA 64A410. The Reynolds number was 4×10^6, and the Mach number was 0.25. The computed pressure coefficients were compared to experimental results,[6] and such a comparison for $\alpha = 6$ deg is shown for a middle cross section in Fig. 2. The combined method solution agreed quite well with the experiment at the root and middle sections of the wing, but there was a notable underestimation of the top surface suction at the tip station. At the tip also the computed results near the trailing edge seem unnatural and different from the experiment. It is likely that this is caused by wing tip vortices and increased spanwise flow that the new method cannot handle. Similar comparisons at a higher angle of attack, $\alpha = 16$ deg, are shown in Fig. 2 for the root and middle sections. Even for such high sweep the solution at wing root (where the assumption of two-dimensional flow is valid) seems remarkably accurate at such a high angle of attack. Yet, at the stations closer to the tip there were some convergence problems with the boundary-layer computation, and it can be seen that the method dramatically overshoots the minimum C_p value. Yet, the results show that for moderate angles of attack even a highly swept wing can be analyzed with this method with good reliability.

Conclusions

The combined three-dimensional viscous/inviscid analysis method introduced in this Note gave reasonably accurate results with a short computational time in the calculated test cases. The method is especially suitable for low-Reynolds-number flows because of its capability of predicting transition and representing laminar separation bubbles. As a tool for analyzing wings, the code is several orders faster than a N–S solver, and creating the surface paneling is much easier a task than generating a three-dimensional volume grid.

However, the method assumes two-dimensional flow at the cross sections where the boundary-layer is computed, which is not realistic at the wing tip, especially on highly swept wings at high angles of attack. Neglecting possible crossflow instabilities can also cause errors in the transition prediction for swept wings. Therefore, the method is limited to only moderate sweep angles, or only low angles of attack for high sweep and is not suitable for small aspect ratio wings. The panel method HISSS breaks down in transonic flow, and XFOIL, on the other hand, only works for subsonic flows. These facts limit the applicable range of the combined method to subsonic flows.

This method can readily be used for analysis of more complex configurations as long as the assumption of two-dimensional flow is not violated on the surfaces analyzed. On bulging bodies or vertical surfaces, only an inviscid solution can be computed, and viscosity will not be taken into account. However, this sort of analysis might still give acceptable results at least for lift because the error in the contribution of a fuselage will not be significant in the integrated results. Analysis of sailplanes or general aviation aircraft are self-evident applications, but the method could also be used for analysis of blended wing body designs and hydrofoils.

References

[1]Pesonen, U., Agarwal, R., and Laine, S., "A Fast and Robust Viscous/Inviscid Interaction Code for Wing Flowfield Calculations," AIAA Paper 99-3139, June 1999.

[2]Drela, M., "XFOIL: An Analysis and Design System for Low Reynolds Number Airfoils," *Low Reynolds Number Aerodynamics*, Springer–Verlag, New York, 1989.

[3]Fornasier, L., "HISSS—A Higher-Order Panel Method for Subsonic and Supersonic Attached Flow About Arbitrary Configurations," Messerschmitt, Rept. LKE122-S-PUB-319, Bölkow, Blohm GmbH, 1987.

[4]Yip, L., and Shubert, G., "Pressure Distributions on a 1- by 3-meter Semispan Wing at Sweep Angles from 0° to 40° in Subsonic Flow," NASA TN D-8307, Dec. 1976.

[5]Kaurinkoski, P., and Hellsten, A., "FINFLO: the Parallel Multi-Block Flow Solver," Helsinki Univ. of Technology, Espoo, Finland, Lab. of Aerodynamics, Rept. A-17, Jan. 1988.

[6]Boltz, F., and Kolbe, C., "The Forces and Pressure Distribution at Subsonic Speeds on a Cambered and Twisted Wing Having 45° of Sweepback, and Aspect Ratio of 3, and a Taper Ratio of 0.5," NASA RM-A52D22, July 1952.

Proposed Mechanism for Time Lag of Vortex Breakdown Location in Unsteady Flows

Ismet Gursul*
University of Bath, Bath, BA2 7AY, United Kingdom

Introduction

EXPERIMENTS show that a time lag of breakdown location is observed in all unsteady flows regardless of the source of the unsteadiness. The dynamic response of breakdown location is similar to that of a first-order system. It is suggested in this Note that the time constant is essentially the same for all of the excitations and that the mechanism of the time lag with respect to the quasi-steady case is universal. This universality may originate from the wave propagation properties of the vortex flows. A simple model of time lag of vortex breakdown location was proposed, and the predictions were compared with the experiments.

The time lag of vortex breakdown location with respect to its variation in the quasi-steady case has been observed for several types of wing motion including pitching, plunging, and rolling. Recently, more detailed observations of the phase lag were made by Atta and Rockwell,[1] LeMay et al.,[2] and others. These studies revealed that, for a periodic pitching motion, vortex breakdown location forms hysteresis loops when plotted as a function of angle of attack because of the time lag of breakdown location. It was also shown that the phase lag increases with increasing reduced frequency, without significant influence of Reynolds number. The response of breakdown location was also studied for transient motions such as a finite ramp pitching motion or plunging motion by Thompson et al.,[3] Reynolds and Abtahi,[4] and others. Similar observations of time lag and hysteresis effects were made for pitch-up and pitch-down motions. It has been found that the response of breakdown location is similar to that of a first-order system. The time constant τ can be estimated from the time history of breakdown location in response to a given unsteady wing/surface motion. The estimated values of the time constant for different types of motion are given by Srinivas et al.[5] and Greenwell and Wood.[6] Although the normalized time constant $\tau U_\infty / c$ is affected by the type and amplitude of the motion, the breakdown location in the static case, and the sweep angle of the wing, it value falls between $\tau U_\infty / c = 1$–2 for slender wings ($\Lambda \geq 70$ deg). By curve fitting to the experimental values of the phase lag for pitching wings, Greenwell and Wood[6] obtained $\tau U_\infty / c = 1.67$. In summary, the time constant can be considered essentially the same for different wing/surface motions as a first approximation.

Recent investigations of vortex breakdown control techniques revealed similar time lags. The measured phase lag of breakdown location with respect to the quasi-steady case is shown in Fig. 1 as a function of the reduced frequency $K = \omega c / 2U_\infty$ for the oscillating leading-edge flaps[7] and leading-edge extensions[8] together with the pitching wings.[2,9] Although there is a larger scatter of data at high frequencies, there is a consistent trend of increasing phase lag with increasing reduced frequency. Several factors may contribute to the data scatter: the breakdown location in the static case; the amplitude of the motion; fluctuations of breakdown location, which are also observed for stationary wings; the number of cycles used for phase averaging; and the method used to calculate the phase lag. With these factors in mind, we do not expect a collapse of data for different motions. The purpose of Fig. 1 is simply to show that the phase lags are similar for α, Λ, and δ variations.

Received 22 May 1999; revision received 17 April 2000; accepted for publication 18 April 2000.

*Reader in Aerospace Engineering, Department of Mechanical Engineering.

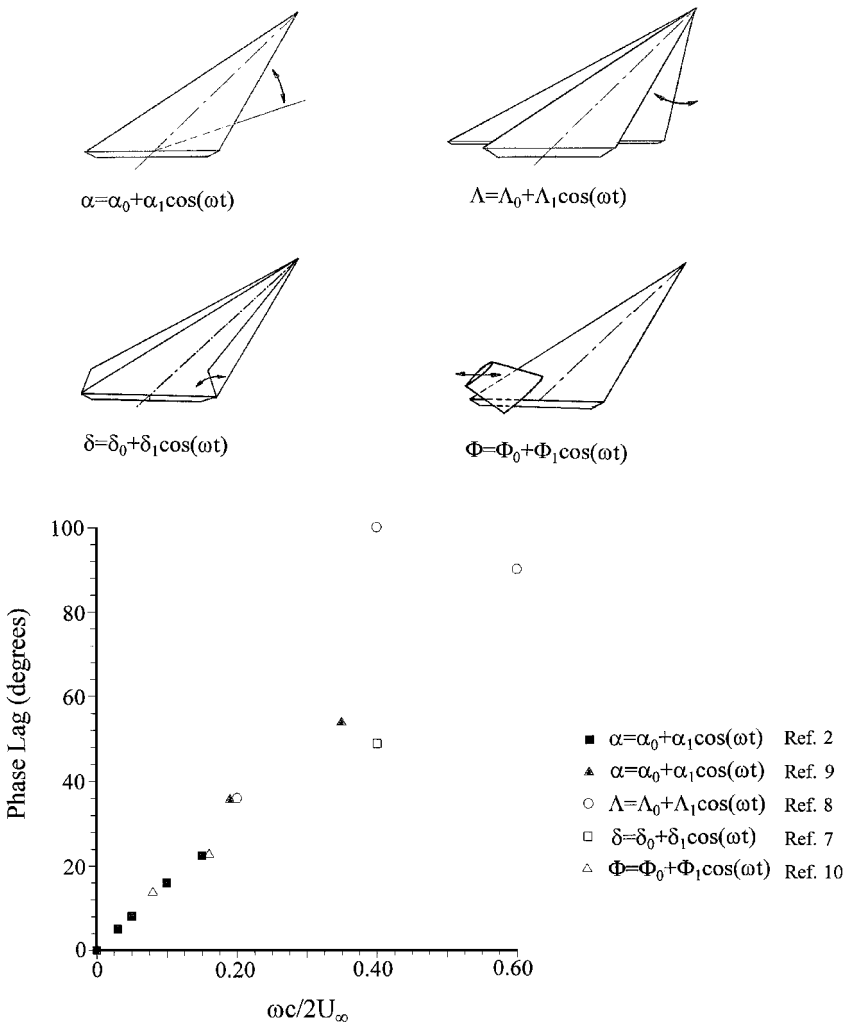

Fig. 1 Phase lag of vortex breakdown location for different types of unsteady motion.

Also shown in Fig. 1 is the phase lag of breakdown location for an oscillating fin placed near the trailing edge of a delta wing.[10] Note that the phase lag agrees very well with that of pitching wings. The effect of the fin oscillations $\Phi(t)$ is expected to be different than that of the other types of motion (shown in Fig. 1) for which the development of the leading edge vortex is time dependent. The flow upstream is steady in this case. Yet, the measured phase lag due to the oscillating fin is very similar. Figure 1 suggests that the mechanism of the time lag is the same regardless of the type of unsteady motion.

Physical mechanism for this phase lag has remained unclear. Note that the observed phase lag of breakdown location is much larger than the time lag in the development of the vortex flow.[11] Greenwell and Wood[6] present a comparison of the time constants (estimated from the surface pressure changes in response to blowing) in the absence and presence of vortex breakdown, which are different by one order of magnitude. Also, if the case of the oscillating fin (shown in Fig. 1) is considered, the upstream flow is free of unsteady effects and there is no time lag in the development of the vortical flow, yet there is considerable time lag of the vortex breakdown location. In another attempt, the observed time lag of breakdown location was explained by the variations of the effective angle of attack and motion-induced longitudinal camber[12] for a pitching delta wing. Both effects are due to the wing motion and fail to explain the phenomenon of the time lag of breakdown location when the wing is stationary. Another explanation for the time lag of breakdown location is the external pressure gradient outside the vortex core, which plays a major role in the dynamic response of breakdown location.[8,9] However, it is not clear how different types of motion or unsteadiness can generate similar phase lags of the external pressure gradient. In this Note, a new explanation of the time lag is proposed. This explanation is based on the wave propagation properties of slender vortex flows.

Proposed Mechanism of Time Lag

One of the well-known explanations of vortex breakdown is based on the wave propagation characteristics of the mean flow, which is measured by the group velocity. Waves may propagate along the vortex core, and the propagation of the waves upstream (against the mean flow) is possible if the flow is subcritical. The wave propagation characteristics may change with streamwise distance along the vortex core. The waves are propagated upstream in the subcritical section, but are unable to propagate farther at a location at which critical conditions exist. This critical location can be taken as an estimate of breakdown location.[13] A stationary breakdown can be considered as the superposition of an upstream moving wave and a uniform freestream velocity (in the downstream direction), which makes the wave stationary. Therefore, the wave speed can be found from the velocity measurements as the negative of the local freestream velocity (axial velocity away from the axis) at the axial position of the stagnation point, as done by Lundgren and Ashurst.[14] The breakdown location can be considered as an equilibrium location at which the local freestream axial velocity W_∞ is equal to the wave speed C_{g0} in the limit of zero axial wave number $k = 0$. When vortex breakdown in unsteady flows is considered, the effect of nonzero frequency (or finite wavelength) should be considered.

The group velocity of the waves traveling upstream depends on the wave number k. For example, in the case of a cylindrical vortex

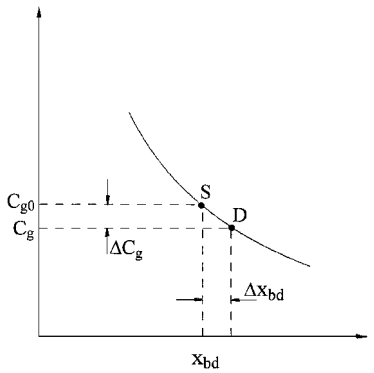

Fig. 2 Vortex breakdown location in static and dynamic conditions.

with the Rankine velocity distribution and no axial velocity, the dispersion relation in the long-wave limit can be approximated as

$$\omega = C_{g0}k[1 + 0.1729(ka)^2 \ln(ka/2)] \quad (1)$$

where ω is the radial frequency and a is the radius of the vortex core. This equation shows that the magnitude of the group velocity $C_g = \partial\omega/\partial k$ decreases with increasing wave number. This result can be also verified from the exact dispersion relation given by Kelvin (see Ref. 10). Therefore, the group velocity C_g for a pitching wing is smaller than the corresponding quasi-steady value C_{g0} by a value ΔC_g. Hence, the equilibrium location (vortex breakdown) is different for the quasi-steady and dynamic cases. For example, the quasi-steady breakdown location (corresponding to an angle of attack $\alpha = \alpha_S$) is shown as S in Fig. 2. At the same angle of attack $\alpha = \alpha_S$, for a pitch-up motion (x_{bd} decreasing), the wave speed is smaller by ΔC_g and, therefore, the equilibrium location is shown as D in Fig. 2. As the angle of attack increases, the breakdown location reaches the location S at a larger angle of attack ($\alpha_U > \alpha_S$). Therefore, for a given breakdown location in the quasi-steady case, a larger angle of attack in pitch-up motion is needed. For the pitch-down motion (x_{bd} increasing), at $\alpha = \alpha_S$, the breakdown location is already at D. At a smaller angle of attack ($\alpha_D < \alpha_U$), the breakdown location will be at S. Therefore, for a given breakdown location in the quasi-steady case, a smaller angle of attack in pitch-down motion is needed. In other words, the vortex breakdown location is aft compared to the quasi-steady case (for a given α) under pitch-up motion and farther forward under pitch-down motion. Hence, the well-known hysteresis effect of breakdown location is explained by using the wave propagation characteristics of the vortex flows. For a periodic pitching motion, an approximate relation between ΔC_g and the phase lag ϕ can be obtained using the static derivatives dC_g/dx_{bd} and $dx_{bd}/d\alpha$.[15] The magnitude of ΔC_g is predicted from the simple model of a cylindrical vortex with the Rankine velocity distribution and no axial velocity.

Experiments

Flow visualization and laser Doppler velocimetry (LDV) measurements in a water tunnel were carried out over a delta wing to determine the static derivatives dC_g/dx_{bd} and $dx_{bd}/d\alpha$ and the phase-averaged variation of breakdown location for a periodic pitching motion. The delta wing model had a sweep angle of $\Lambda = 75$ deg, and the Reynolds number based on the chord length was $Re = 4.1 \times 10^4$ (see Ref. 15 for further details). To determine the static derivative dC_g/dx_{bd}, the wave speed (whose magnitude is equal to the local freestream velocity) was found from the velocity measurements at the axial position of vortex breakdown, as done by Lundgren and Ashurst.[14] The mean angle of attack was $\alpha_0 = 36$ deg, and the amplitude was $\alpha_1 = 4$ deg. The phase angle ϕ was found by using the Fourier's series expansion of the phase-averaged breakdown location.

According to the Rankine vortex model used, the quantity ΔC_g is a function of $\omega/2\Omega$, where Ω is the angular velocity of the vortex core.[10] Therefore, an estimate of Ω is required for this model, which was obtained from the velocity measurements as $\Omega c/U_\infty \cong 7$. By using this estimate, one obtains $\omega/2\Omega = \omega/2(7U_\infty/c) = (\omega c/2U_\infty)/7 = K/7$. The reduction in the wave speed ΔC_g was found as a function of the reduced frequency K and was used to predict the phase lag ϕ. The experimentally measured and predicted phase lags are shown in Fig. 3. The agreement between the experiments and theory is reasonable, considering that the theoretical model is valid for a very simple vortex flow. Also, the model does not take into account the time lag in the development of the vortex flow over the pitching wing. The most important feature of the theoretical model is its capability of predicting phase lags that increase with increasing frequency, which is well known from the experimental observations for a variety of unsteady flows.

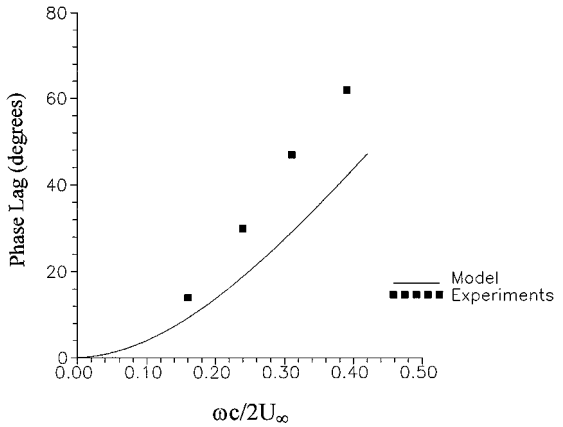

Fig. 3 Variation of phase lag as a function of reduced frequency.

Conclusions

Experiments show that the time constant and phase lag are essentially the same in all unsteady flows regardless of the source of the unsteadiness. This suggests that the mechanism of the time lag with respect to the quasi-steady case is universal. A new explanation based on the wave propagation properties of the vortex flows is proposed. For a pitching motion, well-known hysteresis effects and time lag have been explained with this model. Reasonable agreement between the predicted and measured phase lag was found.

Acknowledgment

The author would like to express his appreciation to Wensheng Xie for his help in the water-tunnel experiments.

References

[1] Atta, R., and Rockwell, D., "Leading-Edge Vortices Due to Low Reynolds Number Flow Past a Pitching Delta Wing," *AIAA Journal*, Vol. 28, No. 6, 1990, pp. 995–1004.

[2] LeMay, S. P., Batill, S. M., and Nelson, R. C., "Vortex Dynamics on a Pitching Delta Wing," *Journal of Aircraft*, Vol. 27, No. 2, 1990, pp. 131–138.

[3] Thompson, S. A., Batill, S. M., and Nelson, R. C., "Separated Flowfield on a Slender Wing Undergoing Transient Pitching Motions," *Journal of Aircraft*, Vol. 28, No. 8, 1991, pp. 489–495.

[4] Reynolds, G. A., and Abtahi, A. A., "Instabilities in Leading-Edge Vortex Development," AIAA Paper 87-2424, Aug. 1987.

[5] Srinivas, S., Gursul, I., and Batta, G., "Active Control of Vortex Breakdown over Delta Wings," AIAA Paper 94-2215, June 1994.

[6] Greenwell, D. I., and Wood, N. J., "Some Observations on the Dynamic Response to Wing Motion of the Vortex Burst Phenomenon," *Aeronautical Journal*, Feb. 1994, pp. 49–59.

[7] Deng, Q., and Gursul, I., "Vortex Breakdown over a Delta Wing with Oscillating Leading Edge Flaps," *Experiments in Fluids*, Vol. 23, No. 4, 1997, pp. 347–352.

[8] Yang, H., and Gursul, I., "Vortex Breakdown over Unsteady Delta Wings and Its Control," *AIAA Journal*, Vol. 35, No. 3, 1997, pp. 571–574.

[9] Gursul, I., and Yang, H., "Vortex Breakdown over a Pitching Delta Wing," *Journal of Fluids and Structures*, Vol. 9, 1995, pp. 571–583.

[10] Xie, W., "An Experimental Investigation of Buffeting Flows over Delta Wings," M.S. Thesis, Dept. of Mechanical Engineering, Univ. of Cincinnati, Cincinnati, OH, Dec. 1998.

[11] Lambourne, N. C., Bryer, D. W., and Maybrey, J. F. M., "The Behaviour of the Leading-Edge Vortices over a Delta Wing Following a Sudden Change

of Incidence," Aeronautical Research Council, R&M 3645, London, March 1969.

[12]Ericsson, L. E., "Pitch Rate Effects on Delta Wing Vortex Breakdown," *Journal of Aircraft*, Vol. 33, No. 3, 1996, pp. 639–642.

[13]Leibovich, S., "Vortex Stability and Breakdown: Survey and Extension," *AIAA Journal*, Vol. 22, No. 9, 1984, pp. 1192–1206.

[14]Lundgren, T. S., and Ashurst, W. T., "Area-Varying Waves on Curved Vortex Tubes with Application to Vortex Breakdown," *Journal of Fluid Mechanics*, Vol. 200, 1989, pp. 283–307.

[15]Gursul, I., "A Proposed Mechanism for the Time Lag of Vortex Breakdown Location in Unsteady Flows," AIAA Paper 2000-0787, Jan. 2000.

Grid Survey Approach to Store Separation Trajectory Prediction

Tan Kok Ching*
DSO National Laboratories,
Singapore 118230, Republic of Singapore

Nomenclature

C_l, C_m, C_n	= rolling, pitching, and yawing moment coefficients
C_{lp}, C_{mq}, C_{nr}	= damping derivative due to roll, pitch, and yaw rates, per radian
C_X, C_Y, C_Z	= axial, side, and vertical force coefficients
X, Y, Z	= longitudinal, lateral, and vertical displacements
α, β	= pitch plane and side-slip angles of attack
α_T	= total angle of attack, $\sqrt{(\alpha^2 + \beta^2)}$
ΔC_{lf}	= incremental C_{lf} due to α and β $[C_{lf(\alpha,\beta)} - C_{lf(\alpha,\beta=0)}]$
ΔC_{mf}	= incremental C_{mf} due to β $[C_{mf(\alpha,\beta)} - C_{mf(\alpha,\beta=0)}]$
ΔC_{nf}	= incremental C_{nf} due to α $[C_{nf(\alpha,\beta)} - C_{nf(\alpha=0,\beta)}]$
ΔC_{Yf}	= incremental C_{Yf} due to $[C_{Yf(\alpha,\beta)} - C_{Yf(\alpha=0,\beta)}]$
ΔC_{Zf}	= incremental C_{Zf} due to β $[C_{Zf(\alpha,\beta)} - C_{Zf(\alpha,\beta=0)}]$
ϕ, θ, ψ	= body axis roll, pitch, and yaw angles

Subscripts

f	= freestream
i	= interference

Introduction

OVER the past years, the advances in computational fluid dynamics (CFD) have greatly encouraged the development of various computational methods for predicting store separation trajectory,[1–3] the motivation being to reduce the engineer's dependence on traditional wind-tunnel tests, which are expensive and time-consuming to use. The present Note attempts to demonstrate the computational prediction of a store separation trajectory, carried out by employing the grid survey approach. The basic grid survey method has been used by engineers to predict store separation trajectory successfully in past decades.[4,5] Typically, a matrix of aerodynamic flowfield data in a region that encompass the anticipated trajectory path of the store are obtained using the captive trajectory system (CTS) in a wind-tunnel facility. A six-degrees-of-freedom (6DOF) program integrates the rigid-body equations of motion by the use of these aerodynamic flowfield data. The present study is based on a similar approach, but an Euler code is used to obtain the flowfield grid data instead of the CTS rig. A case study involving the trajectory of a body–tail store configuration separating from a clipped delta wing at transonic speed of Mach 0.95 is predicted and compared against available CTS results.[6] This test case has also been used by numerous researchers to verify the accuracy of their CFD results in past years.[1–3,7] Figure 1 presents the side view of the configuration with important dimensions illustrated.

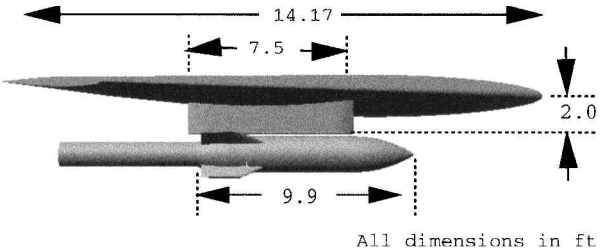

Fig. 1 Configuration geometry (side view).

Formulation

A detailed discussion on the grid survey method may be found in Refs. 4, 5, and 8. The author shall address the key challenge in the grid survey method, which requires the user to prepare the right amount and composition of grid data and apply appropriate aerodynamic modeling to characterize the flowfield of the configuration. The flowfield data required in the grid survey method consist of the freestream and the interference coefficients. The pitch plane freestream coefficients, (C_{Zf} and C_{mf}) are modeled as functions of α, whereas the yaw plane coefficients, (C_{Yf} and C_{nf}) are modeled as functions of β. The interference coefficients, for example, C_{mi} and C_{ni}, which account for the influence of the aircraft on the store are modeled as functions of the Z position relative to the aircraft. Studies have shown that the interference aerodynamics due to other positions (X and Y) and attitudes (ϕ, θ, and ψ) are small and may be neglected.[8] In the present study, these coefficients are obtained using a commercial Euler code, MGAERO.[9] The axial drag coefficient C_{Xf} is modeled as function of α_T, and C_{lf} is treated as zero at all α values. The dynamic derivatives, C_{lp}, C_{mq}, and C_{nr} are estimated using semi-empirical code, MISSILE DATCOM,[10] at $\alpha = 10$ deg, which gives values of -4, -38, and -38, respectively. A simple 6-DOF trajectory simulation program, TRASEP is then used to compute the separation trajectory from the instant of end of stroke, estimated to occur at $t = 0.055$ s, where the slope of the pitch rate of the store reverses in the CTS test. TRASEP is an in-house developed software using SIMULINK[11] under a MATLAB® environment.

From the preliminary result of the first trajectory simulation, the various combinations of α and β experienced by the store at discrete Z positions are obtained. The freestream aerodynamics at these combinations of α and β are then computed using MGAERO to obtain the aerodynamic coupling effect. These secondary effects, for example, ΔC_{lf} and ΔC_{mf}, are modeled as functions of the Z positions and incorporated in the second refined simulation. They are modeled as functions of Z instead of α and β to avoid the need to implement a two-dimensional linear interpolation scheme that would require a substantial increase in grid data. It is assumed that the (α, β) experienced by the store at various Z positions in the second trajectory simulation does not differ very much from the first simulation. The net static aerodynamic coefficients acting on the separating store is equal to the sum total of the freestream (including α–β coupling) and interference coefficients. As an illustration, the net C_m value is represented by the following mathematical expression:

$$C_m(\alpha, Z) = C_{mf}(\alpha) + C_{mi}(Z) + \Delta C_{mf}(Z)$$

Results and Discussion

Flowfield Data

The store-alone aerodynamic data in the pitch plane are computed using MGAERO for α up to 20 deg in steps of 4 deg at Mach

Received 13 August 1999; revision received 25 March 2000; accepted for publication 14 April 2000.

*Senior Member of Technical Staff, Aeronautic Systems Program, 20 Science Park Drive.